NANO LETTERS
Letter
Cite This: Nano Lett. 2019, 19, 5222−5228
pubs.acs.org/NanoLett

Silica Glass Toughened by Consolidation of Glassy Nanoparticles

Yanming Zhang, Liping Huang, and Yunfeng Shi*

Department of Materials Science and Engineering, Rensselaer Polytechnic Institute, 110 Eighth Street, Troy, New York 12180, United States

Supporting Information

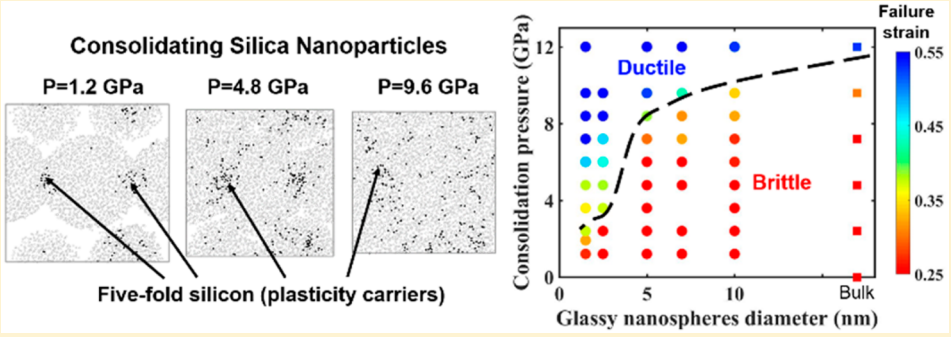

ABSTRACT: The brittleness of oxide glasses has dramatically restricted their practical applications as structural materials despite very high theoretical strength. Herein, using molecular dynamics simulations, we show that silica glass prepared by consolidating glassy nanoparticles exhibit remarkable tensile ductility. Because of dangling bonds at surfaces and high contact stresses, the pressure applied for consolidating glassy nanoparticles to achieve ductility is significantly lower than that required to toughen bulk glass via permanent densification. We have identified 5-fold silicon, with a higher propensity to carry out local shear deformation than 4-fold silicon, as the structural origin for the observed tensile ductility. Interestingly, the work hardening effect has been, for the first time, observed in thus-prepared silica glass, with its strength increasing from 4 GPa to ∼7 GPa upon cold work. This is due to stress-assisted relaxation of 5-fold silicon to 4-fold during cold work, analogous to transformation hardening.

KEYWORDS: *Silica glass, consolidation, brittle to ductile transition, work hardening, 5-fold silicon, molecular dynamics simulation*

Silica glass (SiO_2), with an ultimate strength over 10 GPa for defect-free samples,[1] is believed to be among the strongest materials in the world.[2−5] However, silica glass is difficult to initiate shear flow and exhibits little resistance to crack growth, thus is generally brittle and sensitive to defects.[6−9] Traditional toughening methods, such as thermal tempering or chemical tempering[10] for other oxide glasses, are not suitable for silica glass because its low thermal expansion coefficient and the lacking of mobile ions. Therefore, major development is needed to endow silica ductility to be used as structural materials for load bearing applications.

There are significant research efforts with the aim of toughening silica glass. Electron irradiation during loading has been shown to facilitate bond-switching events to promote plastic deformation.[11] In that case, enhanced plastic deformation is only triggered by active irradiation, which is impossible to achieve in real-world load-bearing situations. The presence of free surfaces has also been shown to elevate the ionic mobility, leading to size-dependent ductility in silica fibers.[12] Recently, silica glass hydrostatically compressed at room temperature has shown both enhanced ductility and high strength when the applied pressure exceeds 10 GPa, according to both experiments and simulations.[13−16] However, it should be emphasized that such high pressure can only be achieved in special designed apparatus such as multianvil cells,[17] where the sample size is limited to several millimeters. Although the critical hydrostatic pressure for the brittle to ductile (BTD) transition could be reduced from 10 to ∼4 GPa if the bulk silica glass is hot compressed near the glass transition temperature (∼1100 °C),[17,18] such processing condition of a combination of high temperature and pressure is extremely challenging to achieve experimentally on a larger scale. Therefore, there is a pressing need to design new processing method with milder thermomechanical conditions to toughen silica glass. To this end, one can use glassy nanoparticles, instead of bulk samples, as starting materials in pressure processing. Consolidating glassy nanoparticles has been explored to form metallic glass systems,[19−22] not yet in oxide glasses experimentally or computationally.

Herein, we used molecular dynamics simulations to prepare tough silica by consolidating glassy nanoparticles instead of bulk samples as in Figure 1a−c. For convenience, silica glass consolidated from glassy nanoparticles is termed consolidated silica (CS). In comparison, silica glass compressed from bulk

Received: April 19, 2019
Revised: June 22, 2019
Published: July 11, 2019

DOI: 10.1021/acs.nanolett.9b01634
Nano Lett. 2019, 19, 5222−5228

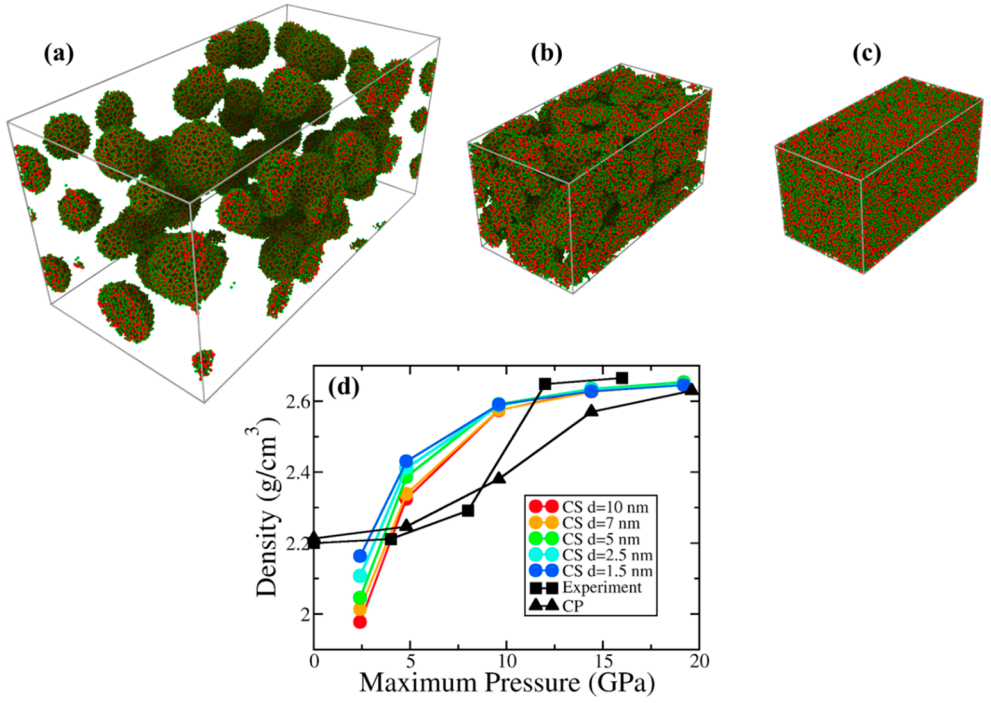

Figure 1. (a–c) Illustration of consolidation of glassy nanoparticles. Oxygen and silicon atoms are colored green and red, respectively. The average nanoparticle diameter is 5 nm. The size of the final consolidated sample (c) is $10 \times 20 \times 10$ nm^3. (d) The density of silica under ambient condition (zero pressure and 300 K), as a function of the maximum pressure during consolidation or compression. CS samples consolidated from glassy nanoparticles with different diameters are shown as filled circles. CP samples compressed from bulk silica are shown as black triangles (MD simulations) and black squares (experiments[15]).

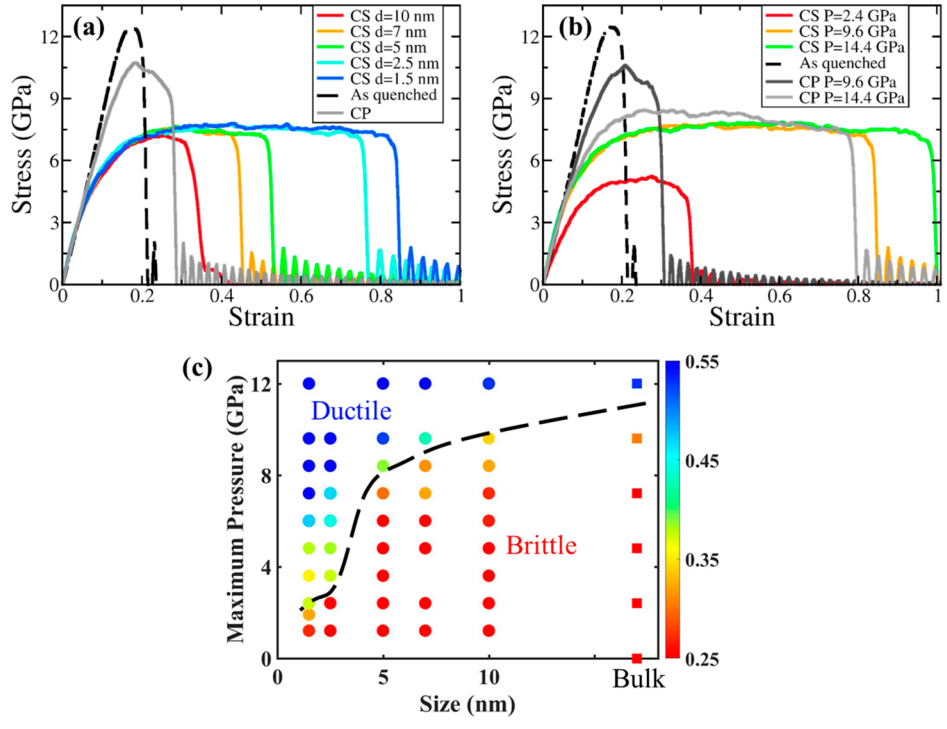

Figure 2. (a) Stress–strain curves of CS and CP samples and as quenched silica glass under uniaxial tension tests. Both CS samples with different average diameters and CP samples are prepared with a maximum hydrostatic pressure of 9.6 GPa. (b) Stress–strain curves of CS and CP samples prepared with different hydrostatic pressures at 300 K under uniaxial tension tests. The average diameter of glassy nanoparticles is ~1.5 nm for CS samples. (c) Ductility map (in terms of failure strain) of CS samples (solid circles) as a function of nanoparticles size and the maximum hydrostatic pressure. CP samples (solid squares) are also shown here for comparison. The failure strain is color-coded from red (0.25) to blue (0.55). The dashed line indicates the BTD transition with a critical failure strain of 35%.

DOI: 10.1021/acs.nanolett.9b01634
Nano Lett. 2019, 19, 5222–5228

as-quenched sample is termed compressed silica (CP). The details of sample preparation can be found in the Method section. First, we measured the final density of silica prepared under different hydrostatic pressures at room temperature after returning back to zero pressure. It is well-known that bulk silica glass can be densified under hydrostatic pressure,[23] and permanent densification occurs as pressure exceeds ~10 GPa in bulk glass.[13,24,25] As shown in Figure 1d, ~20% density increase can be obtained in consolidated silica glass around 20 GPa regardless of the preconsolidated state, in agreement with experiment observations.[15,17,26] Interestingly, consolidated silica from glassy nanoparticles displays higher density at the relatively low-pressure regime, particularly with smaller nanoparticles as starting materials.

We further investigated mechanical responses of consolidated silica from nanoparticles by carrying out uniaxial tension tests. The as-quenched silica glass was also tested for comparison, which behaves in a manner similar to that reported in previous simulation results albeit using different force field.[27−29] Figure 2a shows the stress−strain curves of a number of consolidated silica samples prepared with different starting materials up to the same consolidation pressure of 9.6 GPa. It appears that the Young's moduli of different samples are almost identical. Surprisingly, consolidated silica from glassy nanoparticles displays exceptional ductility which reaches up to ~80% failure strain and increases as the nanoparticles size reduces. The significant plastic deformation inside consolidated silica is shown in Figure S1. In contrast, the compressed silica exhibits only marginally enhanced plasticity with a failure strain of ~29%. Therefore, the utilization of silica nanoparticles as the starting material for consolidation is effective for toughening.

Figure 2b shows the stress−strain curves of a number of CS and CP samples prepared using different hydrostatic pressures. The Young's moduli of most of the samples are very close, except the one that contains pores prepared at the lowest consolidation pressure. It is shown that for the CP samples, as applied pressure increases, the sample becomes more ductile, yet weaker in strength. Prepared at room temperature, enhanced mechanical properties can only be achieved for bulk silica glass (CP samples) when applied pressure exceeds ~10 GPa, consistent with existing literatures.[23,16,25] However, it should be emphasized that a relatively low pressure (~2.4 GPa) is sufficient to achieve considerable ductility (~40%) for CS samples by room-temperature consolidation despite the presence of pores inside. As consolidation pressure increases, the sample becomes more ductile and stronger.

We further systematically investigate the effect of nanoparticle size and consolidation pressure on the ductility of silica samples by mapping out the complete size-pressure-ductility map. As shown in Figure 2c, each CS glass, prepared from certain pressure at 300 K, is represented by a colored solid circle according to its failure strain. For comparison, CP samples are also shown as colored solid squares. Across all samples, there is a brittle-to-ductile (BTD) transition as the consolidation pressure increases. The critical consolidation pressure decreases for CS samples with smaller glassy nanoparticles. If one uses 35% failure strain as the threshold value for the BTD transition, the critical consolidation pressure is around 2 GPa for ~1.5 nm glassy nanoparticles, which is significantly lower than 10 GPa for bulk silica. Thus, by utilizing glassy nanoparticles for consolidation, one can reduce 5-fold the critical consolidation pressure to synthesize tough silica glass at room temperature.

We have conducted tensile loading−unloading-reloading test on a CS sample, similar to the testing protocol on work hardening effect for a polycrystalline metal.[30] As shown in Figure 3, the yield strength of the original CS sample is about 4

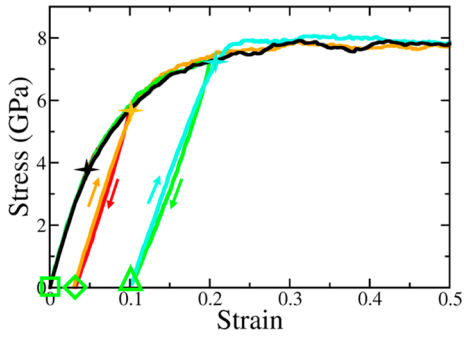

Figure 3. Stress vs strain curves from strain−control loading−unloading−reloading uniaxial tension test for a CS sample. The CS sample is prepared from 19.2 GPa and 300 K with D_{ave} = ~7 nm. Stars mark the yield points for the CS sample and the cold-worked samples. The original CS sample, the 10% cold-worked sample and the 20% cold-worked sample are highlighted by the green square, diamond and triangle.

GPa under uniaxial tension test. Alternatively, the original CS sample was first loaded to 10% engineering strain in tension (following the black line up to 10%) and then unloaded to zero stress completely (red line). Permanent plastic deformation occurs as the sample without load is now 3% longer along the loading direction. The cold-worked sample is then uniaxially loaded up to 50% strain as shown by the orange line. The yield strength now becomes ~6 GPa, indicating significant hardening. One can also repeat the cold work protocol with a higher strain (20%), as shown by the green and cyan curves, resulting in elevating the yield strength to almost 7 GPa, almost twice as the initial glassy sample. It should be mentioned that similar work hardening behavior was also observed for CP samples. Thus, there is a common structural origin for work hardening in these samples, independent of the starting material for consolidation.

To understand the structural origin for the enhanced ductility observed in consolidated silica, we focused on the 5-fold silicon atoms (i.e., silicon atoms with five oxygen neighbors that are within a cutoff distance of 0.215 nm). Liang[16] has shown that the 5-fold silicon atoms and plastic events are highly correlated, given that the occurrence of plastic events for densified silica glass under shear test is signaled by the population peak of 5-fold silicon. Yuan[18] further proposed that 5-fold silicon atoms are more easily to experience shear deformation since they have less rigid local environments. However, there has been no quantitative understanding of both the correlation between tensile ductility and 5-fold silicon atoms population in silica glass and the easiness of shear flow for 5-fold silicon atoms. To tackle the issue, we employed a sample preparation procedure in Figure S2 to generate a variety of silica samples consolidated at different temperatures (8 different temperatures between 300 and 2100 K), and different pressure (11 different pressure between 1.2 and 19.2 GPa) to obtain samples with different 5-fold silicon population. We used two different nanoparticles

DOI: 10.1021/acs.nanolett.9b01634
Nano Lett. 2019, 19, 5222−5228

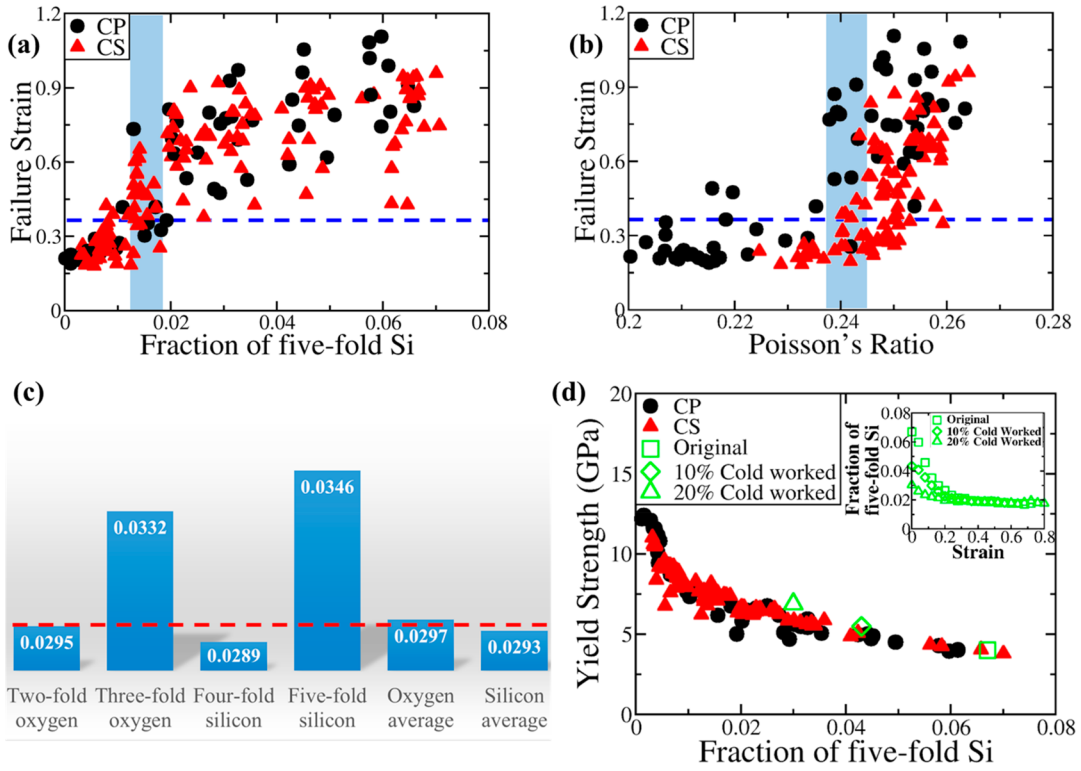

Figure 4. (a) Failure strain versus 5-fold Si population for both CS and CP samples generated following the procedure in Figure S2; two different nanoparticle sizes D_{ave} = 2.5 and 7 nm are used to prepare CS samples. (b) Poisson's ratio versus failure strain for both CS and CP samples. The blue dashed line labels the BTD transition boundary using a critical failure strain of 35%. (c) The average shear strain of different groups of atoms in a CS sample, upon a loading−unloading cycle with a maximum tensile strain of 5%. The red dash line indicates the average shear strain of the entire sample. (d) Yield strength versus 5-fold Si population for CS, CP, and cold worked samples. The inset shows population of 5-fold silicon atoms reduce upon uniaxial tension test for the original CS sample (green square), the 10% cold-worked sample (green diamond), and the 20% cold worked sample (green triangle).

(CS samples with D_{ave} = ∼7 nm and D_{ave} = ∼2.5 nm) as well as bulk silica (CP samples), as the starting material for consolidation, which will then be subjected to uniaxial mechanical tests. It should be noted that the presence of pore affects the mechanical properties of the consolidated glass. To show the effect only from 5-fold silicon, without the interference from the pores, we excluded samples containing pores larger than ∼1.5 nm (the pore size calculation follows Gelb and Gubbin[31]). In this way, one can delineate the correlation between structure (in terms of 5-fold silicon population) and ductility (in terms of failure strain). Figure 4a shows the failure strain of consolidated silica as a function of the 5-fold silicon fraction, showing a positive correlation. This general trend seems insensitive to the starting materials, indicating the applicability of 5-fold silicon fraction as a universal structural parameter for the ductility of silica glass. For consolidated silica with more than 2% 5-fold silicon, the samples are ductile, and vice versa. In addition, for various consolidated silica glass, we also observe a positive correlation between failure strain and Poisson's ratio, which has been linked to the fracture energy as shown in both experiments and simulations.[27,32,33] Specifically, samples with a Poisson's ratio higher than ∼0.25 are ductile, while brittle when the Poisson's ratio is lower than 0.24 as seen in Figure 4b. Therefore, the critical Poisson's ratio for the BTD transition for silica glass observed here agrees very well with previous reports.[18,27] It is interesting to note that Rouxel and co-workers have shown that experimental densified silica can reach a Poisson's ratio of ∼0.25, which is able to flow under indentation.[34] This densified glass in experiment agrees well with our consolidated silica samples in the domain of Poisson's ratio and density (Figure S3). Encouragingly, the plasticity carriers in such densified silica is stable, or quenchable from compression in experimental time scales.

Next, to understand mechanistically the role 5-fold silicon atoms play in the deformation of consolidated silica, we conducted statistical analysis on the shear deformation propensity of atoms with different coordination environment. To calculate shear deformation propensity, a CS sample (identical to the one used in Figure 3) was subjected to uniaxial tensile loading to 5% strain and then unload to zero stress. The sample sustains a permanent elongation of about 1% due to plastic deformation. The average shear strain of all atoms after the loading−unloading process is 2.96% (the averaged shear strain is slightly higher for oxygen than silicon) as in Figure 4c. In comparison, 5-fold silicon atoms have an average shear strain of 3.46%, ∼20% higher than that of 4-fold silicon atoms. Closely related 3-fold oxygen atoms (bonded to three silicon atoms within 0.215 nm) have an average shear strain of 3.32%, ∼12.5% higher than that of 2-fold oxygen atoms. Therefore, both 5-fold silicon and 3-fold oxygen atoms are plasticity carriers in consolidated silica glass, which leads to the BTD transition as their population increases. This is analogous to the liquid-like regions in amorphous silicon[35] or metallic glasses,[36−38] which give rise to apparent shear deformation. It should be noted that the 3-fold oxygen population is highly correlated to 5-fold silicon population, such that there is no need to consider them separately.

DOI: 10.1021/acs.nanolett.9b01634
Nano Lett. 2019, 19, 5222−5228

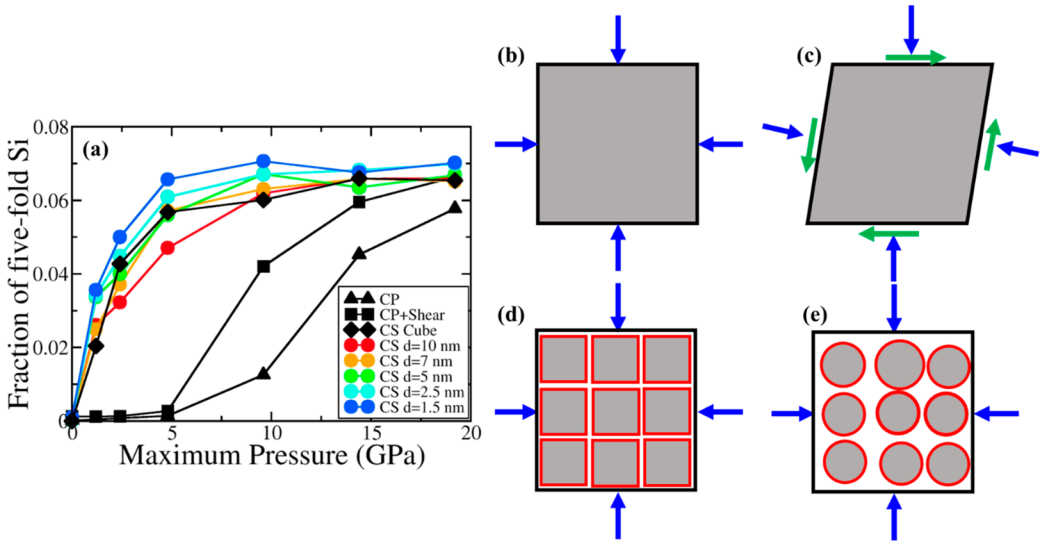

Figure 5. (a) Five-fold silicon fraction as a function of consolidation pressure for different consolidated silica with various starting materials: CP sample under hydrostatic stress (b), CP sample under hydrostatic and shear stress (c), CS sample with glassy nanocubes (d), and CS samples with different sizes of spherical glassy nanoparticles (e).

As 5-fold silicon atoms are energetically less stable than 4-fold silicon at ambient condition, these 5-fold silicon atoms may undergo structural transition back to 4-fold silicon under favorable thermomechanical conditions. Upon plastic deformation, 5-fold silicon can transit to 4-fold in a process similar to stress-assisted structural relaxation[39] as shown in inset of Figure 4d. The 5-fold silicon fractions of the samples prior to mechanical tests are 6.7% (original CS sample), 4.3% (10% cold-worked), and 3.0% (20% cold-worked). Importantly, lower 5-fold silicon population leads to higher yield strength for both CP and CS samples as shown in Figure 4d. In other words, the stress-assisted structural relaxation of 5-fold silicon to 4-fold silicon is responsible for the work-hardening of consolidated silica glass. It is important to examine the stability of 5-fold silicon (Figure S4). Without any load, the 5-fold silicon population of the sample stabilizes at ∼0.5%, ∼1% when annealing at 900 and 600 K with zero pressure, respectively. We fully anticipate the stable population of 5-fold silicon at ambient condition is above 1%. Therefore, 5-fold silicon, once formed under high pressure, is not only quenchable to the ambient condition but is sufficiently stable against elevated temperature.

Lastly, we investigated why glassy nanoparticles are superior starting materials that lead to low critical consolidation pressure for the BTD transition (as shown in Figure 2). This question is equivalent to, according to the structural origin of the BTD transition shown in Figure 4, why glassy nanoparticles are better starting materials in promoting 5-fold silicon formation during consolidation. Figure 5a shows the 5-fold silicon fraction as a function of different consolidation pressure for a number of different starting materials. 5-fold silicon atoms form more readily during consolidating glassy nanoparticles than bulk silica (black triangles), particularly for those with smaller glassy nanoparticles. In addition, the distribution of 5-fold silicon atoms are more homogeneous as pressure increases as shown in Figure S5. Particularly, 5-fold silicon atoms mostly locate at contact area among nanospheres when the applied pressure is low. Two factors may contribute to the formation of 5-fold silicon in consolidated silica: high local shear stresses at particle−particle contacts and large amount of surface area with dangling bonds. To isolate these two effects, we first compared the consolidated bulk silica with (Figure 5c) and without shear (Figure 5b). The presence of 2 GPa of shear stress promotes 5-fold silicon formation (∼3-fold increase at 10 GPa consolidation pressure) for bulk silica samples, as shown in Figure 5a. This is analogous to the observation that shear promotes permanent densification reported earlier.[40] Next, we used cube-shaped silica nanoparticles (∼6 nm in size) as the starting materials for consolidation, in which dangling bonds exist yet without high contact shear stress (contacts are between flat surfaces). It can be seen that the consolidated cube-shaped nanoparticles sample contains large amount of 5-fold silicon. The presence of free surfaces and dangling bonds elevates the free energy of the initial state prior to 5-fold silicon formation during consolidation and, thus, lowers the activation energy barrier for the 4-fold to 5-fold silicon transition under pressure.

In conclusion, we prepared silica glass with enhanced ductility by the consolidation of glassy nanoparticles. The remarkable tensile ductility up to 100% observed in consolidated silica is originated from the formation of considerable amount of 5-fold silicon atoms. The most intriguing advantage about this method is that a much lower pressure (2.4 GPa) is required to achieve apparent ductility (∼40%) for silica glass at room temperature, whereas over 10 GPa is needed by applying traditional processing method like cold compression of bulk silica. The significant reduction of critical pressure to trigger the BTD transition can be attributed to contact shear stress and dangling bonds at nanoparticle surfaces which promote 5-fold silicon formation during consolidation. In addition, interesting work hardening effect has been observed in consolidated silica glass, in which case the yield strength increases from ∼4 GPa to ∼7 GPa upon cold working, owing to stress-assisted relaxation of 5-fold silicon atoms to 4-fold silicon atoms during deformation. We believe this work could help design new processing routes to achieve ductile oxide glasses and enable broad applications of oxide glasses as structural materials.

Method. Classical molecular dynamic simulations were carried out in LAMMPS package[41] (https://lammps.sandia.

DOI: 10.1021/acs.nanolett.9b01634
Nano Lett. 2019, 19, 5222−5228

gov/) using a modified version of the Buckingham potential.[42] It has been shown that this potential can accurately reproduce the structure and mechanical properties of silica glass under hydrostatic pressure.[42] The short-range cutoff is 0.8 nm. The long-range Columbic cutoff is 1.0 nm. The long-range Columbic interaction was calculated via the Wolf truncation method[43] to increase the computational efficiency. The equations of motion were integrated by Velocity−Verlet algorithm with a time step of 1.6 fs. Nosé−Hoover barostat and thermostat[44,45] were used to control the pressure and temperature of the system.

Bulk silica glass samples were quenched isobarically under zero pressure from well-equilibrated high temperature (3600 K) melt to room temperature (300 K) with a rate about 4 K/ps. Polydisperse glassy nanoparticles are then carved from this bulk glass, with a size sampled from a uniform distribution around an average diameter D_{ave} (from ∼1.5 to ∼10 nm) with a half-width of 1 nm. The glassy nanoparticles are shifted randomly away from a simple cubic lattice to avoid overlapping, as well as artificial periodicity. The entire simulation box is subjected to a room- temperature consolidation following a pressure profile in Figure S2. The consolidation process can be seen in Figure 1. Depending on the initial nanoparticle size, the resulting glassy sample after consolidation is around 10 nm by 20 nm by 10 nm (with atoms population ranging from 155 754 to 239 865 atoms), except for the sample with D_{ave} = 10 nm which is around 15 nm by 30 nm by 15 nm with 588 108 atoms. The sample is sufficiently long and not slender enough to trigger the known size/shape effect.[46,47] We have tested sample that is twice as long in loading direction, which exhibits identical mechanical responses as in Figure S6a. Uniaxial tension test was then carried out under 300 K with an engineering strain rate of 2.5 ns^{-1}. The mechanical response of a silica sample seems not sensitive to the strain rate in the test range as shown in Figure S6b. Periodic boundary conditions were applied in all three directions. The visualization software OVITO[48] was used to generate simulation snapshots, animations and local atomic strain/stress was calculated based on method proposed by Falk and Langer.[49]

■ ASSOCIATED CONTENT

Supporting Information

The Supporting Information is available free of charge on the ACS Publications website at DOI: 10.1021/acs.nanolett.9b01634.

Shear strain distribution for as quenched glass, compressed silica, and consolidated silica during uniaxial tension test, schematic diagram of the consolidation route, mapping of CP and CS samples, as well as experimental densified silica, in the domain of the Poisson's ratio and density at ambient condition, evolution of five-fold silicon atoms population, distribution of five-fold silicon atoms within 1 nm layer for silica glass, and stress−strain curves under uniaxial tension test at different sample sizes and strain rates (PDF)

■ AUTHOR INFORMATION

Corresponding Author

*E-mail: shiy2@rpi.edu.

ORCID

Yanming Zhang: 0000-0001-7810-3825

Yunfeng Shi: 0000-0003-1700-6049

Notes

The authors declare no competing financial interest.

■ ACKNOWLEDGMENTS

This work was supported by the National Science Foundation under Grants DMR-1508410 and 1255378. We would like to thank Dr. Shiv Prakash Singh from Karlsruhe Institute of Technology, Professor Ravishankar Sundararaman, Dr. Siddharth Sundararaman, Swastik Basu, and Haidong Liu from Rensselaer Polytechnic Institute for useful discussions. The simulations were carried out in the Center for Computational Innovations (CCI) at Rensselaer.

■ REFERENCES

(1) Brambilla, G.; Payne, D. N. *Nano Lett.* **2009**, *9* (2), 831−835.
(2) Brückner, R. *J. Non-Cryst. Solids* **1970**, *5* (2), 123−175.
(3) Huang, L.; Durandurdu, M.; Kieffer, J. *Nat. Mater.* **2006**, *5* (12), 977−981.
(4) Lawn, B. R.; Hockey, B. J.; Wiederhorn, S. M. *J. Mater. Sci.* **1980**, *15* (5), 1207−1223.
(5) Daguier, P.; Nghiem, B.; Bouchaud, E.; Creuzet, F. *Phys. Rev. Lett.* **1997**, *78* (6), 1062−1065.
(6) Rountree, C. L.; Kalia, R. K.; Lidorikis, E.; Nakano, A.; Van Brutzel, L.; Vashishta, P. *Annu. Rev. Mater. Res.* **2002**, *32* (1), 377−400.
(7) Célarié, F.; Prades, S.; Bonamy, D.; Ferrero, L.; Bouchaud, E.; Guillot, C.; Marlière, C. *Phys. Rev. Lett.* **2003**, *90* (7), No. 075504.
(8) Chen, Y. C.; Lu, Z.; Nomura, K.; Wang, W.; Kalia, R. K.; Nakano, A.; Vashishta, P. *Phys. Rev. Lett.* **2007**, *99* (15), No. 155506.
(9) Basu, S.; Koratkar, N.; Shi, Y. *Acta Mater.* **2019**, *175*, 11−20.
(10) Wondraczek, L.; Mauro, J. C.; Eckert, J.; Kühn, U.; Horbach, J.; Deubener, J.; Rouxel, T. *Adv. Mater.* **2011**, *23* (39), 4578−4586.
(11) Zheng, K.; Wang, C.; Cheng, Y.-Q.; Yue, Y.; Han, X.; Zhang, Z.; Shan, Z.; Mao, S. X.; Ye, M.; Yin, Y.; et al. *Nat. Commun.* **2010**, *1* (3), 1−8.
(12) Luo, J.; Wang, J.; Bitzek, E.; Huang, J. Y.; Zheng, H.; Tong, L.; Yang, Q.; Li, J.; Mao, S. X. *Nano Lett.* **2016**, *16* (1), 105−113.
(13) Wakabayashi, D.; Funamori, N.; Sato, T.; Taniguchi, T. *Phys. Rev. B: Condens. Matter Mater. Phys.* **2011**, *84* (14), No. 144103.
(14) Wakabayashi, D.; Funamori, N.; Sato, T. *Phys. Rev. B: Condens. Matter Mater. Phys.* **2015**, *91* (1), No. 014106.
(15) Rouxel, T.; Ji, H.; Hammouda, T.; Moréac, A. *Phys. Rev. Lett.* **2008**, *100* (22), No. 225501.
(16) Liang, Y.; Miranda, C. R.; Scandolo, S. *Phys. Rev. B: Condens. Matter Mater. Phys.* **2007**, *75* (2), No. 024205.
(17) Guerette, M.; Ackerson, M. R.; Thomas, J.; Yuan, F.; Watson, E. B.; Walker, D.; Huang, L. *Sci. Rep.* **2015**, *5*, 15343.
(18) Yuan, F.; Huang, L. *Sci. Rep.* **2015**, *4*, 5035.
(19) Wang, X.; Jiang, F.; Hahn, H.; Li, J.; Gleiter, H.; Sun, J.; Fang, J. *Scr. Mater.* **2016**, *116*, 95−99.
(20) Danilov, D.; Hahn, H.; Gleiter, H.; Wenzel, W. *ACS Nano* **2016**, *10* (3), 3241−3247.
(21) Gleiter, H. *Acta Mater.* **2000**, *48* (1), 1−29.
(22) Gleiter, H. *Small* **2016**, *12* (16), 2225−2233.
(23) Huang, L.; Kieffer, J. *Appl. Phys. Lett.* **2006**, *89* (14), 141915.
(24) Mantisi, B.; Tanguy, A.; Kermouche, G.; Barthel, E. *Eur. Phys. J. B* **2012**, *85* (9), 304.
(25) Huang, L.; Kieffer, J. *Phys. Rev. B: Condens. Matter Mater. Phys.* **2004**, *69* (22), No. 224204.
(26) Polian, A.; Grimsditch, M. *Phys. Rev. B: Condens. Matter Mater. Phys.* **1990**, *41* (9), 6086−6087.
(27) Shi, Y.; Luo, J.; Yuan, F.; Huang, L. *J. Appl. Phys.* **2014**, *115* (4), 043528.
(28) Pedone, A.; Malavasi, G.; Menziani, M. C.; Segre, U.; Cormack, A. N. *Chem. Mater.* **2008**, *20* (13), 4356−4366.

DOI: 10.1021/acs.nanolett.9b01634
Nano Lett. 2019, 19, 5222−5228

(29) Yuan, F.; Huang, L. *J. Non-Cryst. Solids* **2012**, *358* (24), 3481−3487.
(30) Wu, Y.; Xiao, Y.; Chen, G.; Liu, C. T.; Lu, Z. *Adv. Mater.* **2010**, *22* (25), 2770−2773.
(31) Gelb, L. D.; Gubbins, K. E. *Langmuir* **1999**, *15* (2), 305−308.
(32) Lewandowski, J. J.; Wang, W. H.; Greer, A. L. *Philos. Mag. Lett.* **2005**, *85* (2), 77−87.
(33) Deng, B.; Shi, Y. *J. Appl. Phys.* **2018**, *124* (3), 035101.
(34) Rouxel, T.; Ji, H.; Guin, J. P.; Augereau, F.; Rufflé, B. *J. Appl. Phys.* **2010**, *107* (9), 094903.
(35) Demkowicz, M. J.; Argon, A. S. *Phys. Rev. B: Condens. Matter Mater. Phys.* **2005**, *72* (24), 245206.
(36) Shi, Y.; Katz, M. B.; Li, H.; Falk, M. L. *Phys. Rev. Lett.* **2007**, *98* (18), 185505.
(37) Shi, Y.; Falk, M. L. *Acta Mater.* **2007**, *55* (13), 4317−4324.
(38) Shi, Y.; Falk, M. L. *Scr. Mater.* **2006**, *54* (3), 381−386.
(39) Wang, Z. T.; Pan, J.; Li, Y.; Schuh, C. A. *Phys. Rev. Lett.* **2013**, *111* (13), No. 135504.
(40) Mackenzie, J. D. *J. Am. Ceram. Soc.* **1963**, *46* (10), 461−470.
(41) Plimpton, S. *J. Comput. Phys.* **1995**, *117* (1), 1−19.
(42) Sundararaman, S.; Huang, L.; Ispas, S.; Kob, W. *J. Chem. Phys.* **2018**, *148* (19), 194504.
(43) Wolf, D.; Keblinski, P.; Phillpot, S. R.; Eggebrecht, J. *J. Chem. Phys.* **1999**, *110* (17), 8254−8282.
(44) Nosé, S. *J. Chem. Phys.* **1984**, *81* (1), 511−519.
(45) Nosé, S. *Mol. Phys.* **1984**, *52* (2), 255−268.
(46) Şopu, D.; Foroughi, A.; Stoica, M.; Eckert, J. *Nano Lett.* **2016**, *16* (7), 4467−4471.
(47) Shi, Y. *Int. Mater. Rev.* **2019**, *64*, 163.
(48) Stukowski, A. *Modell. Simul. Mater. Sci. Eng.* **2010**, *18* (1), 015012.
(49) Falk, M. L.; Langer, J. S. *Phys. Rev. E: Stat. Phys., Plasmas, Fluids, Relat. Interdiscip. Top.* **1998**, *57* (6), 7192−7205.

DOI: 10.1021/acs.nanolett.9b01634
Nano Lett. 2019, 19, 5222−5228